Research Article | Vol. 11, No. 9 / 1 September 2020 / Biomedical Optics Express 4915
Biomedical Optics EXPRESS

# Liquid crystal–photopolymer composite films for label-free single-substrate protein quantitation and immunoassay

MON-JUAN LEE,[1,2,4] FEI-FAN DUAN,[3] PO-CHANG WU,[3] AND WEI LEE[3,5]

[1]Department of Bioscience Technology, Chang Jung Christian University, Guiren Dist., Tainan 71101, Taiwan
[2]Department of Medical Sciences Industry, Chang Jung Christian University, Guiren Dist., Tainan 71101, Taiwan
[3]Institute of Imaging and Biomedical Photonics, College of Photonics, National Chiao Tung University, Guiren Dist., Tainan 71150, Taiwan
[4]mjlee@mail.cjcu.edu.tw
[5]wlee@nctu.edu.tw

**Abstract:** Conventional liquid crystal (LC)-based biosensing at the LC–glass interface requires the assembly of an LC cell formed by two glass substrates with an LC film sandwiched in between. As most biochemical and clinical assays are performed on a single solid substrate, the feasibility of a single-substrate biodetection platform based on a thin film of LC–photopolymer composite was explored in this study. The LC mixture, consisting of nematic LC, E7 or AY40-006, doped with a small amount ($\leq 5$ wt%) of a photocurable prepolymer was spin-coated on a glass substrate modified with dimethyloctadecyl[3-trimethoxysilyl)propyl] ammonium chloride (DMOAP), a vertical alignment reagent, followed by irradiation with ultraviolet (UV) light. During the photopolymerization process, the accumulated and polymerized NOA65 at the LC–glass interface weakened the anchoring strength of DMOAP, resulting in a decrease in the pretilt angle of LC and allowing the LC molecules to be more easily disturbed in the presence of biomolecules, compared with vertically aligned LC in the absence of polymerized NOA65. Incorporating NOA65 in the LC film therefore provides a means for signal amplification. When an LC–photopolymer composite film consisting of AY40-006 and 4-wt% NOA65 was exposed to UV at 15 mW/cm$^2$ for 30 s and utilized as the biosensing mesogen, the limits of detection were $1.6 \times 10^{-12}$ g/ml for the direct detection of bovine serum albumin (BSA) and $2.1 \times 10^{-8}$ g/ml for the immunoassay of the cancer biomarker CA125, significantly lower than those detected with AY40-006 alone or AY40-006/NOA65 mixture without UV irradiation. The results from this study offer a compelling implication on the biomedical application of LC–photopolymer composites in label-free and single-substrate biodetection.



## 1. Introduction

Conventional label-based biochemical and clinical assays, such as enzyme-linked immunosorbent assay (ELISA) and western blot analysis, usually require secondary antibodies labeled with chromophores, fluorophores, or enzymes to bring about colorimetric, fluorescence or chemiluminescence signals. Because of the cross-reactivity of the secondary antibodies, which often leads to nonspecific or false-positive results, such indirect detection methods are being replaced by direct detection or label-free methods, in which the specific binding between the target of detection and the capture molecule, such as the immunoreaction between an antigen and an antibody, can be detected directly by electrical, optical, or electrochemical means. Over the past decade or more, various label-free biosensing technologies based on liquid crystals (LCs)

#398858 https://doi.org/10.1364/BOE.398858
Journal © 2020 Received 15 Jun 2020; revised 30 Jul 2020; accepted 30 Jul 2020; published 7 Aug 2020

Biomedical Optics EXPRESS

have been developed [1]. These include biodetection at the LC–glass interface, which usually involves a thin film of LC sandwiched between two glass substrates to construct an LC cell, and at the LC–aqueous interface in the form of LC films or LC-in-water droplets. The biosensing potential of both categories of LCs, thermotropic and lyotropic LCs, has been demonstrated, but most LC-based biosensors reported to date utilize the nematic 5CB as the sensing mesogen [2,3]. As a wide variety of LC materials are available commercially and extensively applied industrially, exploring the potential of LCs other than 5CB in biosensing is essential to enhance the performance and extend the capabilities of current LC-based biodetection methods [4].

Composite materials of polymer and LC are extensively studied for their unique properties and potential applications in various electro-optical devices. Polymer-stabilized LC (PSLC) and polymer-dispersed LC (PDLC) are among the most well-studied LC–polymer composites. PSLC is formed by embedding a polymer network amid orderly aligned LC molecules. The amount of polymer is usually less than 10 wt% in a typical PSLC [5], in contrast to PDLC, which comprises LC droplets dispersed in a polymeric matrix with a much higher polymer content [6]. By incorporating polymer, PSLC and PDLC composites with unique dielectric and electro-optical properties are created, with intriguing advantages such as shorter response time over pristine LCs [7–10]. Therefore, both PSLC and PDLC have been actively investigated in the development of fast-switching devices such as electrochromic films, flexible displays, and switchable smart windows [6,11,12].

In this study an LC–photopolymer composite film with a relatively lower polymer content than PSLC and PDLC was applied in the development of a label-free and LC-based biosensing technology on a single glass substrate. As label-based bioassays such as ELISA and western blot, as well as label-free biodetection techniques, say, surface plasmon resonance (SPR) are performed on a single substrate of glass, plastic or membrane, the tedious procedure imposed by the assembly of an LC cell is relatively unfavorable, except when an electric field is required for detection [13–17]. Since LC-based biosensing relies on the disruption of orderly aligned LC molecules in the presence of biomolecules at the LC–glass interface, the polymer content or the level of photopolymerization in the LC–photopolymer composite film is preferably lower than those in PSLC and PDLC so that the initial orientation of LCs in the absence of the target of detection is not significantly affected by the polymer. On the other hand, the isotropic polymer may provide a new means for signal amplification, which is one of the technical concerns in label-free biosensing based on LC as a probe. Our previous studies have shown that the optical signal derived from the interaction of LCs with biomolecules can be enhanced by employing a nematic LC of large optical anisotropy or high birefringence [18–20], by modifying the vertically aligning reagent with ultraviolet (UV) irradiation to increase binding affinity [18], by aligning the direction of linearly polarized light with the rubbing direction of the glass substrate [21], or by subjecting LC to a weak electric field [14].

Here an LC–photopolymer composite film for biosensing purpose was synthesized by incorporating a minute amount of the photocurable prepolymer Norland Optical Adhesive 65 (NOA65) in the nematic LC E7 or AY40-006. The single-substrate biodetection platform was designed so that the director or long axis of LC molecules in the LC–photopolymer composite film was aligned perpendicularly to the glass substrate as well as at the LC–air interface. The glass surface was chemically modified with the homeotropic alignment reagent, dimethyloctadecyl[3-trimethoxysilyl)propyl] ammonium chloride (DMOAP), to provide the vertical anchoring force, while air also tends to align LCs homeotropically so that in the absence of biomolecules the optical texture was dark when observed under a polarizing optical microscope (POM) with crossed polarizers. Disturbance in LC alignment caused by biomolecules at the LC–glass interface can be detected by the optical signal of light leakage significantly enhanced by photopolymerized NOA65. The performance of the single-substrate biosensing platform based on the LC–photopolymer probe was assessed by the limit of detection (LOD) of bovine serum albumin (BSA), a common

Biomedical Optics EXPRESS

protein standard, at various concentrations of NOA65 exposed to various UV intensities to control the extent of polymerization. An immunoassay for the cancer biomarker CA125 was also demonstrated as a proof-of-concept of the feasibility of the technology in cancer screening. Results from this study provide insights to single-substrate biodetection and signal amplification at the LC–glass interface by employing an LC–photopolymer composite film.

## 2. Materials and methods

### 2.1. Materials

The NEG AT35 (22 × 18 × 1.1 mm) optical glass substrates were purchased from Ruilong Glass, Miaoli, Taiwan. The vertical alignment agent, DMOAP, received as 60% in methanol, was purchased from Acros Organics (Thermo Fisher Scientific, Waltham, MA, USA). The LC–photopolymer composite used in this study was prepared from the nematic LC E7 (having birefringence $\Delta n = 0.2255$ at a wavelength of 589 nm and temperature of 20 °C and possessing the clearing point $T_c$ of 61 °C for the nematic–isotropic phase transition) or AY40-006 ($\Delta n = 0.249$ at a wavelength of 589.3 nm and temperature of 20 °C and exhibiting the isotropic phase at $T_c = 90$ °C and beyond). They are products of Daily Polymer Corp., Kaohsiung, Taiwan, and Bayi Space, Beijing, China, respectively. NOA65, a liquid prepolymer that facilitates the formation of photopolymer upon UV irradiation, was manufactured by Norland Products, Inc. (Cranbury, NJ, USA). The protein standard BSA was obtained from Sigma–Aldrich (St. Louis, Missouri). The recombinant human CA125/MUC16 and anti-CA125 antibodies were produced by R&D Systems and Santa Cruz Biotechnology, respectively. The protein and antibody were stored at conditions suggested by the manufacturers and diluted in sterilized DI water to desired concentrations before experiment.

### 2.2. Preparation of DMOAP-coated glass substrates

The optical glass substrates were immersed in a detergent solution and sonicated for 15 min, followed by sonication twice in DI water for 15 min and once in ethanol for 15 min. The cleaned glass slides were baked at 74 °C to remove residual ethanol. DMOAP was diluted in DI water to 1% (v/v) and reacted with cleaned glass slides at room temperature with sonication for 15 min. The DMOAP-coated glass substrates were then washed twice by sonicating in DI water for 15 min. After being blown dry with nitrogen, the glass slides were baked at 85 °C for 15 min.

### 2.3. LC-based single-substrate protein assay

As illustrated in Fig. 1, BSA solution at a designated concentration was dispensed with a Gilson Pipetman G P20G micropipette at 3 $\mu$l/spot on a DMOAP-coated glass substrate to form a 2 × 2 protein array, followed by drying at 30 °C for 30 min. After rinsing with DI water to remove nonadsorbed BSA, an LC film was formed by adding a mixture of E7/NOA65 or AY40-006/NOA65 to the DMOAP-coated and then BSA-immobilized glass substrate, followed by spin-coating at 1000 rpm for 10 s and subsequently at 5000 rpm for another 10 s. The LC film was then irradiated with UV light of 365 nm in wavelength at a uniform intensity of 5–20 mW/cm$^2$ for 30 s to promote the photopolymerization of NOA65. UV irradiation was performed with a Panasonic Aicure UJ35 LED Spot Type UV Curing System. The UV light source was situated 20 cm above the glass substrate (Fig. 1(e)). The average LC film thickness was 4.5 ± 0.5 $\mu$m as measured by interferometry. The optical texture of LCs was observed with an Olympus BX51 POM (Tokyo, Japan) with crossed polarizers in the transmission mode, and POM images were captured with an Olympus XC30 digital camera mounted on the microscope.

Biomedical Optics EXPRESS

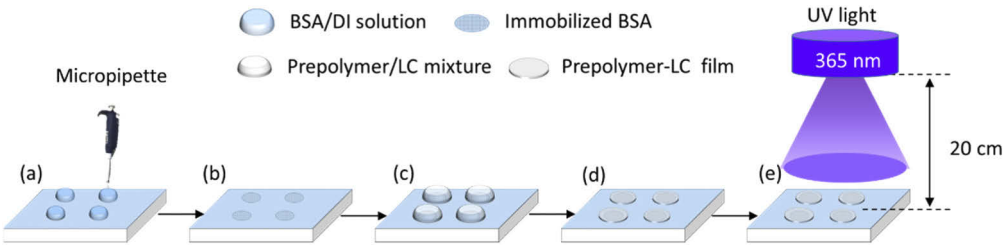


**Fig. 1.** Schematic of the LC-based single-substrate protein assay. (a) BSA solution was dispensed at 3 $\mu$l/spot on a DMOAP-coated glass substrate, followed by (b) drying at 30 °C for 30 min and rinsing with DI water to obtain immobilized BSA. (c) The LC–photopolymer composite film was formed by dispensing a mixture of LC/NOA65 on the BSA-immobilized substrate, followed by (d) spin-coating at 1000 rpm for 10 s and then at 5000 rpm for another 10 s to obtain the LC film, which was (e) irradiated with UV light at an intensity of 5–20 mW/cm$^2$ for 30 s.

### 2.4. LC-based single-substrate CA125 immunoassay

An aqueous solution of anti-CA125 antibody was dispensed successively at 5 $\mu$l/spot on a DMOAP-coated glass substrate to form a $2\times2$ antibody array. After drying at 30 °C for 30 min, 20 $\mu$l of an aqueous solution of CA125 at a designated concentration was dispensed on the immobilized anti-CA125 antibody, followed by covering the glass substrate with a cover glass so that the entire glass surface was in contact with the CA125 protein solution. After reacting for 30 min, the glass substrate was rinsed with DI water to remove unbound CA125. The AY40-006/NOA65 mixture was then spin-coated on the glass substrate as described in Section 2.3.

### 2.5. Image analysis with the GIMP software

The brightness of the optical texture images of the LC–photopolymer composite film at various BSA or CA125 concentrations was determined by the GNU Image Manipulation Program (GIMP), version 2.10.14. Prior to image analysis, the POM images were resized to a quarter of the original file with the aspect ratio maintained. The RGB values (0–255) of each pixel in a defined circular area with a radius of 120 pixels were then summed to represent the relative intensity of the optical texture. At least 3 repeated experiments were performed to calculate the average and standard deviation of the relative intensity at each BSA or CA125 concentration. The standard deviation $s$ used in the calculation of LOD was obtained from at least 7 repeated experiments.

## 3. Results and discussion

### 3.1. Effect of NOA65 concentration and UV intensity on the initially vertical alignment of E7 and AY40-006

The single-substrate biosensing platform was designed by establishing an LC–photopolymer thin film on a glass substrate dip-coated with a vertically aligning surfactant. E7 and AY40-006 were individually mixed with NOA65, followed by spin-coating and UV irradiation on DMOAP-covered glass substrates to render two types of LC–photopolymer composite films for comparison. Doping LCs with low concentrations ($\leq$ 5 wt%) of NOA65 would not alter the phase sequence of E7 and AY40-006, for which the nematic phase is the only mesophase that exists in a wide temperature range including the room temperature. The NOA65 concentration and UV intensity were optimized to control the extent of polymerization of the prepolymer such that, in the absence of biomolecules at the LC–glass interface, the photopolymer-containing LCs

Biomedical Optics EXPRESS

remained undisturbed in the homeotropic state. This allows biomolecules to be readily detected when a dark-to-bright transition in the optical texture appears, which serves as the signal for the disrupted LC orientation caused by the biomolecular target of detection.

At concentrations of NOA65 ranging from 3 to 5 wt%, E7 and AY40-006 exhibited a completely dark texture prior to UV exposure when observed under the POM with crossed polarizers, indicating that both LCs were vertically aligned (upper panels, Figs. 2(a) and 2(b)). However, when exposed to UV at an intensity of 10 mW/cm$^2$ for 30 s, the optical texture of both E7 and AY40-006 turned bright for the samples with 5-wt% NOA65 (lower panels, Figs. 2(a) and 2(b)). On the other hand, when the NOA65 concentration was fixed at 3 wt% followed by UV exposure with intensities ranging from 0 to 20 mW/cm$^2$ for 30 s, both the E7 and AY40-006 composites exhibited a bright background signal at 20 mW/cm$^2$ (Fig. 3). In order to avoid such background signal in the absence of biomolecules, the concentration of NOA65 used in the synthesis of the LC–photopolymer composites was lowered to 4 wt% or less, whereas the UV intensity was limited to 15 mW/cm$^2$ or less in the following studies.

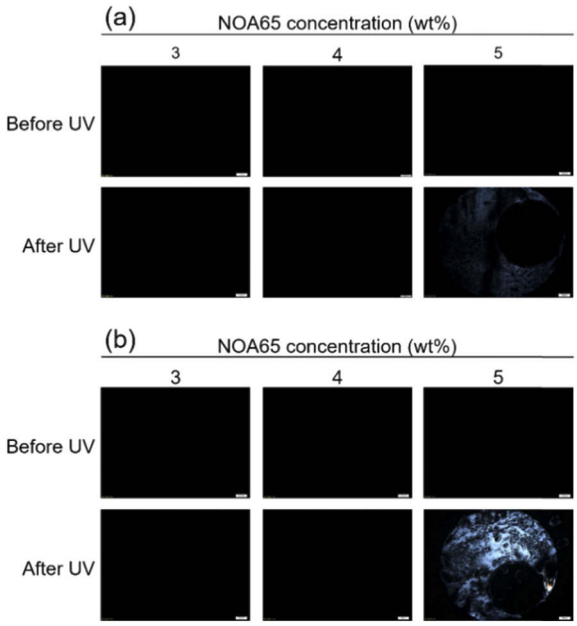


**Fig. 2.** Optical textures of the LC–photopolymer composite films at various concentrations of NOA65 before and after UV exposure. The LC–photopolymer composite film was formed by mixing either (a) E7 or (b) AY40-006 with NOA65 at a designated concentration, followed by its spin-coating on a DMOAP-coated glass substrate and successive UV irradiation at 10 mW/cm$^2$ for 30 s. Scale bar: 100 $\mu$m.

It is known that NOA65 tends to accumulate and becomes polymerized at the LC–glass interface during photopolymerization through phase separation when the content of NOA65 is low ($\leq$ 5 wt%) in an LC–prepolymer blend, resulting in gravel- or network-like morphologies suggestive of an increase in surface roughness [22,23]. On a vertically aligned cell composed of two polyimide-coated substrates, the pretilt angle (measured from the substrate plane) of E7 and the total surface energy have been reported to decrease with increasing NOA65 concentration (0.5–2.5 wt%) under a 25-mW/cm$^2$ UV exposure for 50 min [23]. It is inferred from these previous findings that the surface anchoring strength on DMOAP in the present study was weakened with the increase in polymerized NOA65 at the LC–glass interface so that LC molecules were no longer aligned homeotropically, giving rise to light scattering and an enhanced background signal

Biomedical Optics EXPRESS

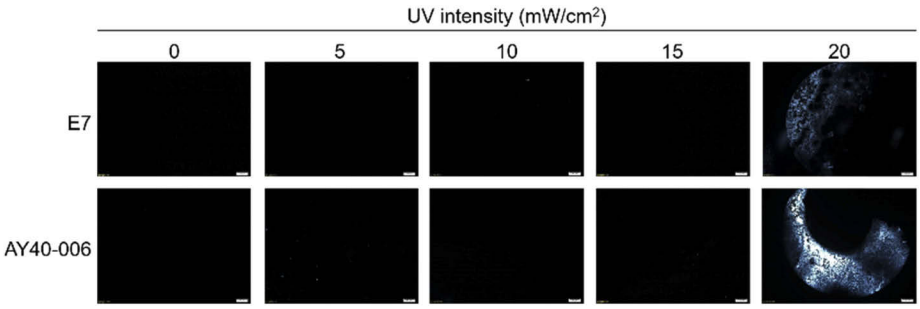


**Fig. 3.** Optical textures of the LC–photopolymer composite films formed at various UV intensities. The LC–photopolymer composite was prepared by mixing either E7 or AY40-006 with 3-wt% NOA65, followed by spin-coating on a DMOAP-coated glass substrate and subsequently by UV irradiation for 30 s at various designated UV intensities. Scale bar: 100 $\mu$m.

at a higher NOA65 concentration (5 wt%) or UV intensity (20 mW/cm$^2$) as shown in Figs. 2 and 3. Obviously, by carefully controlling the level of polymerization, it is possible to manipulate or reduce the surface anchoring energy of LCs, thereby facilitating signal amplification in the presence of the analyte at the LC–glass interface.

### 3.2. *Protein assay with the single-substrate detection platform based on the LC–photopolymer composite film*

When BSA was immobilized on the DMOAP-coated glass substrate, a dark-to-bright transition with increasing BSA concentrations was observed in the optical textures of the composite films formed by both E7 and AY40-006 doped with 3-wt% NOA65 prior to UV irradiation (upper panels, Figs. 4(a) and 4(b)). Compared with the completely dark background in the absence of BSA, the minimal BSA concentration with discernible brightness was $10^{-9}$ and $10^{-10}$ g/ml for the E7/NOA65 and AY40-006/NOA65 films, respectively. After UV exposure at an intensity of 10 mW/cm$^2$ for 30 s, optical signals were favorably observed at lower concentrations, $10^{-10}$ and $10^{-11}$ g/ml for the respective E7/NOA65 and AY40-006/NOA65 films (lower panels, Figs. 4(a) and 4(b)). The uneven distribution of protein sample on the DMOAP-coated glass substrate is a result of the coffee ring effect [24]. During the drying procedure (30 °C, 30 min), water evaporating from the edge of the droplet of the protein solution is replenished by that from the interior, resulting in an outward flow carrying the protein solute to the edge of the droplet, thus forming a ring stain.

Quantitative results, expressed as relative intensities from image analysis of the optical textures with the GIMP software, were plotted against BSA concentration to provide a calibration curve for protein assay, a common practice in biochemical protein quantitation (Figs. 4(c) and 4(d)). A protein assay utilizing BSA as the protein standard is designed to be non-selective against different types of proteins, because the assay is used to determine the total protein concentration of a sample. Since we rely on calibration curves for quantitative analysis, the protein samples are not expected to stay in the original concentration on the glass substrate, as long as all protein standards and analytes are processed in the same way. In other words, after 3 $\mu$l of $10^{-6}$ g/ml BSA was dried at 30 °C for 30 min, followed by rinsing and spin-coating of the LC–photopolymer composite film, the relative intensity of the corresponding LC optical texture is representative of $10^{-6}$ g/ml BSA (or 3 ng BSA), even though water was evaporated. To determine the concentration of an unknown protein analyte, one can immobilize the same volume (3 $\mu$l) of the analyte on a DMOAP-coated glass substrate as that of the BSA standards, followed by detection with the LC

Biomedical Optics EXPRESS

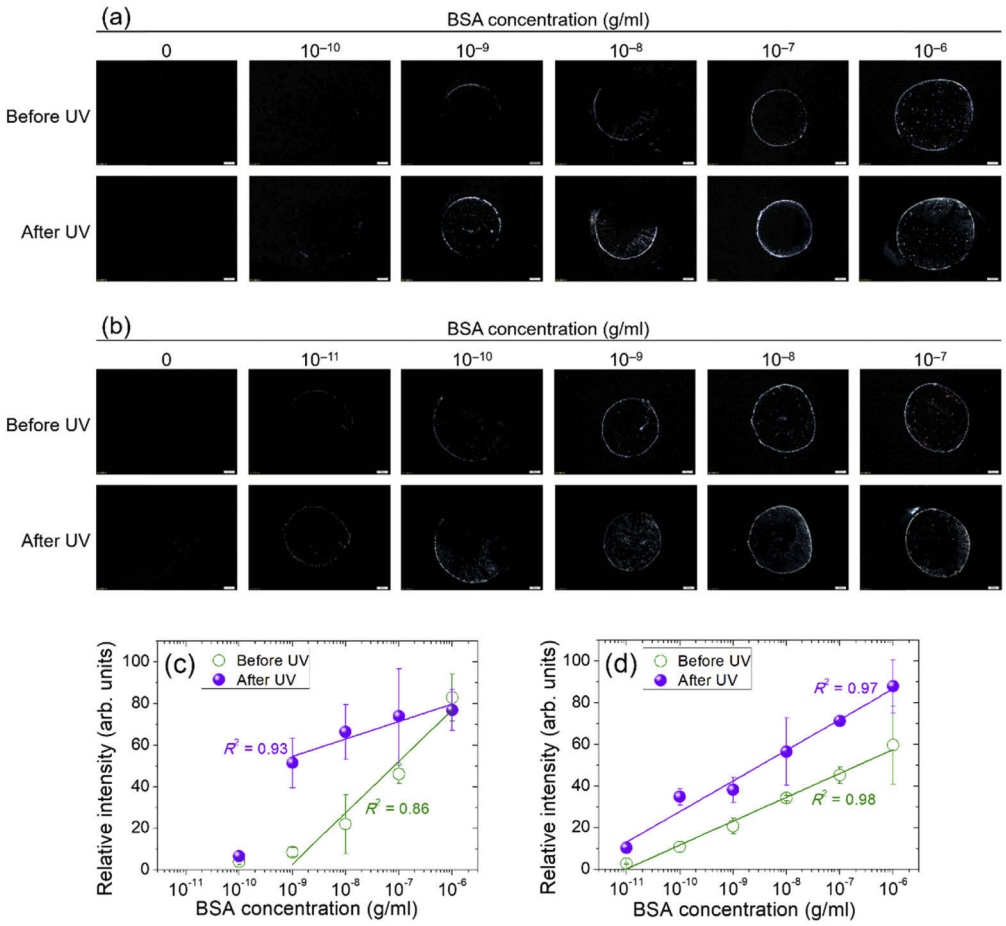


**Fig. 4.** Optical textures of LC–photopolymer composite films in the presence of various concentrations of BSA and the corresponding quantitative results. The LC–photopolymer composite film was formed by mixing either (a) E7 or (b) AY40-006 with 3-wt% NOA65, followed by spin-coating and UV irradiation at 10 mW/cm$^2$ for 30 s. Scale bar: 100 $\mu$m. Quantitative results from image analysis of the optical textures with the GIMP software are expressed as relative intensities plotted against the BSA concentration in (c) the E7/NOA65 platform and (d) the AY40-006/NOA65 platform. Error bars represent standard deviations calculated from the relative intensities of at least three independent experiments. Solid lines represent the fitted linear regression lines, with the coefficient of determination, $R^2$, indicated in the same color.

film. The concentration of the unknown protein analyte can then be determined by interpolating its relative intensity in a calibration curve such as those in Figs. 4(c) and 4(d).

In Figs. 4(c) and 4(d), the relative intensity of E7 and AY40-006 after UV exposure was higher than that without photopolymerization, suggesting that polymerized NOA65 avails signal amplification. This can be explained by the reduced anchoring strength caused by polymerized NOA65 on the surface to permit the initially and vertically ordered LC molecules to become more easily disturbed, producing light leakage in the presence of BSA compared with pristine LC or LC/NOA65 mixtures prior to UV irradiation, in which LCs are vertically aligned by the strong anchoring force from DMOAP. Furthermore, the enhanced optical signal was also a result of severe index mismatch arising from the randomized LC orientations, creating LC multidomains

Biomedical Optics EXPRESS

with domain boundaries to enhance light scattering. To evaluate the performance, LOD was calculated using the equation $3s/m$, where $s$ is the standard deviation of the relative intensity at the lowest BSA concentration with discernible brightness in the optical texture and $m$ is the slope of the calibration curve [25]. The thus-obtained LOD for the AY40-006/NOA65 film was $2.8 \times 10^{-10}$ g/ml, which was an order of magnitude lower than that of $1.8 \times 10^{-9}$ g/ml for the E7/NOA65 film in BSA detection.

To determine whether UV irradiation alone would affect the BSA detection, neat LC counterparts were prepared (without NOA65) by spin-coating and then exposed to UV at 15 mW/cm$^2$ for 30 s. For both pure E7 and AY40-006 films, the brightness of the optical texture was unaffected by UV exposure (Fig. 5), supporting that the signal amplification observed in Fig. 4 resulted from the photopolymerization of NOA65. It is worth mentioning that, on the other hand, when NOA65 was substituted with the reactive mesogen RM257 (Merck), the induced photopolymerization enabled by the photoinitiator IRG184 (BASF) of 0.5 wt% under UV irradiation at 20 mW/cm$^2$ for 120 s did not lead to observable amplification of light leakage induced by the immobilized BSA interfaced with E7 (data not shown). This result implies that the formation and morphological characteristics of the photopolymer, as reported in [22], is critical to signal amplification. Inferably, instead of the polymeric fibril network distributed among LCs, it was the phase separation and accumulation of NOA65 induced by photopolymerization at the LC–glass interface, as evidenced by the scanning electron microscopic images in the literature [22,23], that accounted for the light-amplification effect.

We next fine-tuned the protein assay by increasing the weight percentage of NOA65 to 4 wt% in the AY40-006/NOA65 mixture and studied the effect of UV intensity on the LOD of the LC–photopolymer composite film thus formed. Without photopolymerization, the LOD of AY40-006/NOA65 at 4 wt% NOA65 (before UV irradiation, Fig. 6(a)) was similar to that at 3 wt% (before UV, Fig. 4(b)), which in both cases were $10^{-10}$ g/ml of BSA. When exposed to UV

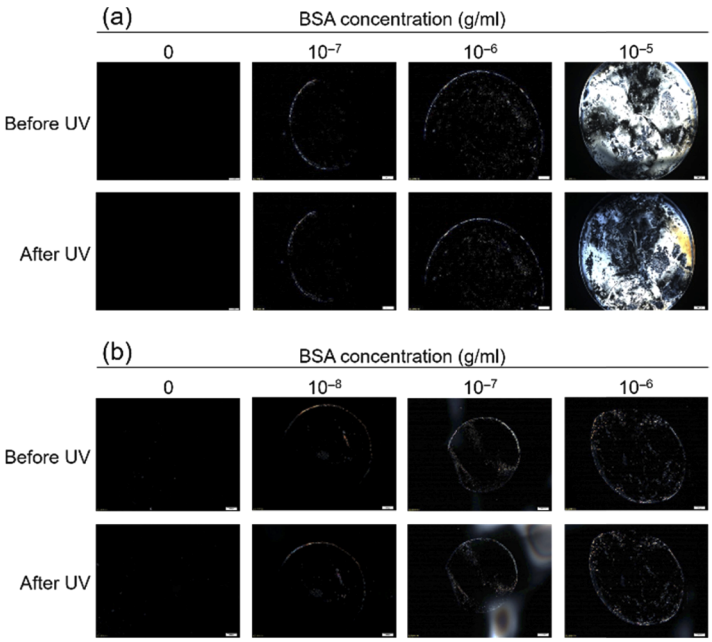


**Fig. 5.** Optical textures of LC films before and after exposure to UV in the presence of various concentrations of BSA. The LC film was formed by spin-coating pristine (a) E7 or (b) AY40-006, followed by UV irradiation at 15 mW/cm$^2$ for 30 s. Scale bar: 100 $\mu$m.

Biomedical Optics EXPRESS

at 5 mW/cm$^2$ for 30 s, the brightness of the optical texture resembled that before UV irradiation (Fig. 6(a)). Nevertheless, when the UV intensity was increased to 10 and 15 mW/cm$^2$, there was a significant decrease in LOD to $1.9 \times 10^{-11}$ and $1.6 \times 10^{-12}$ g/ml of BSA, respectively (Figs. 6(a) and 6(b)). Because of the enhanced background signal at an NOA65 concentration of 5 wt% and a UV intensity of 20 mW/cm$^2$ in the absence of BSA (Figs. 2 and 3), we considered 4-wt% NOA65 and 15-mW/cm$^2$ UV exposure for 30 s the optimized conditions for the preparation of the AY40-006/NOA65 platform.

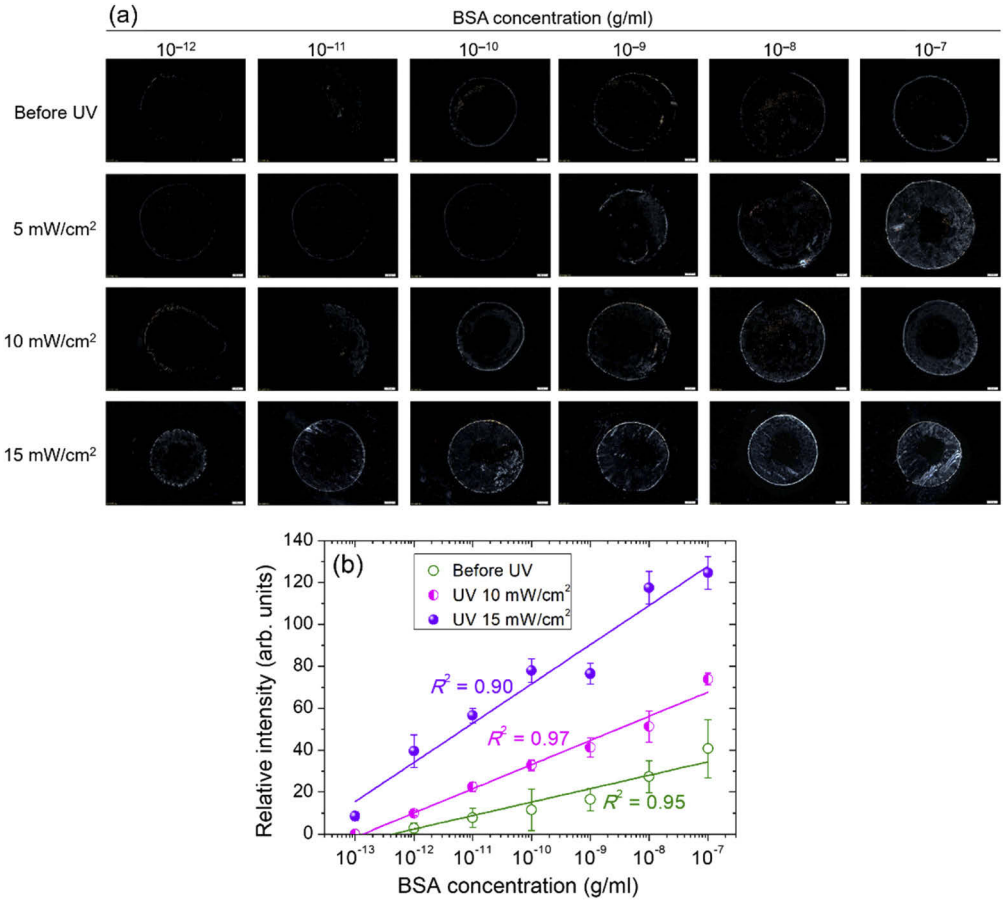


**Fig. 6.** Effect of UV intensities on the optical textures of the LC–photopolymer composite film in the presence of various concentrations of BSA. (a) The LC–photopolymer composite film was formed by mixing AY40-006 with 4-wt% NOA65, followed by spin-coating and subsequent UV irradiation for 30 s at 5, 10, or 15 mW/cm$^2$. Scale bar: 100 $\mu$m. (b) Quantitative results from image analysis of the optical textures with the GIMP software are expressed as the relative intensity as a function of the BSA concentration. Error bars represent standard deviations calculated from the relative intensities of at least three independent experiments. Solid lines represent the fitted linear regression lines, with the coefficient of determination, $R^2$, indicated in the same color.

Biomedical Optics EXPRESS

### 3.3. CA125 immunoassay with the single-substrate detection platform based on the LC–photopolymer composite film

The potential for clinical application of the single-substrate biodetection platform based on the LC–photopolymer composite film was manifested in an immunoassay for the cancer biomarker CA125. The immunoassay was established by first immobilizing anti-CA125 antibodies on the DMOAP-coated glass substrate, followed by reacting the entire glass surface, including areas without anti-CA125 antibodies, with various concentrations of CA125. The immunocomplex thus formed was then detected with an LC–photopolymer composite film of NOA65 (4 wt%)-impregnated AY40-006 exposed to UV radiation at 15 mW/cm$^2$ for 30 s. To avoid false-positive signals, the amount of immobilized anti-CA125 antibodies was adjusted so that the antibodies would not disrupt the vertical alignment of LCs and that the optical texture remained dark in the absence of CA125. As depicted in Fig. 7, the dark-to-bright transition of the optical texture of pristine AY40-006 occurred at an anti-CA125 antibody concentration of $10^{-7}$ g/ml, while that of AY40-006/NOA65 occurred at $10^{-9}$ g/ml. Accordingly, to detect CA125 with the AY40-006 or the AY40-006/NOA65 film, the immobilized antibody concentrations were limited in this work to 0.01 $\mu$g/ml and 0.1 ng/ml, respectively, which correspond to 0.05 ng/spot and 0.5 pg/spot of antibodies at 5 $\mu$l/spot in a $2 \times 2$ antibody array.

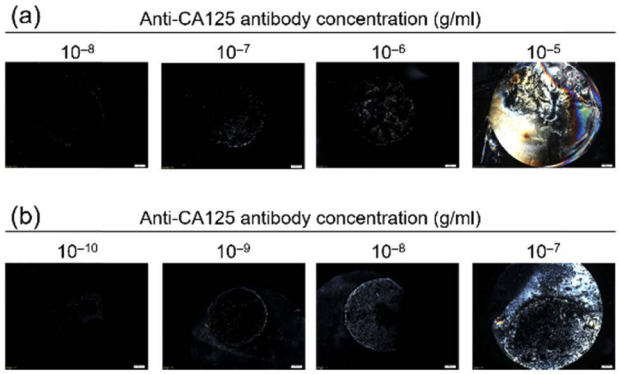


**Fig. 7.** Optical textures of the (a) LC and (b) LC–photopolymer films in the presence of various concentrations of immobilized anti-CA125 antibodies. The LC and LC–photopolymer composite films were formed by spin-coating (a) AY40-006 alone without UV exposure and (b) a mixture of AY40-006 and 4-wt% NOA65 followed by UV irradiation at 15 mW/cm$^2$ for 30 s, respectively. Scale bar: 100 $\mu$m.

Because the amount of immobilized anti-CA125 antibodies was controlled, ensuring AY40-006 to stay vertically aligned (Fig. 7), the light leakage observed in the presence of CA125 can then be attributed to the formation of the CA125/anti-CA125 immunocomplex (Fig. 8). By reacting CA125 with the entire glass substrate, both specific and nonspecific interactions can be examined. Optical responses occurring within the circular area immobilized with anti-CA125 antibodies are specific, while those observed outside the circular area are non-specific. In Figs. 8(a) and 8(b), the dark background in the peripheral area without the immobilized anti-CA125 antibody suggests that within the range of CA125 concentration examined, the extent of nonspecific adsorption of CA125, if occurred, was not significant enough to alter the orientation of LCs or to induce a nonspecific optical response. Furthermore, the specificity of the immunoreaction was demonstrated by substituting anti-CA125 antibodies for other nonspecific antibodies, and no optical response was observed when the nonspecific antibody was reacted with CA125 [19]. Similarly, when CA125 was replaced by BSA, the optical texture of LC remained dark in the area immobilized with anti-CA125 antibodies [21]. As one can see in Fig. 8(a), when 0.01

Biomedical Optics EXPRESS

$\mu$g/ml of anti-CA125 antibody was immobilized, the lowest CA125 concentration detected by the AY40-006 film was $10^{-7}$ g/ml. As for the AY40-006/NOA65 film, a calculated LOD of $2.1 \times 10^{-8}$ g/ml for CA125 was achieved when a much lower concentration of anti-CA125 antibody, 0.1 ng/ml, was immobilized (Figs. 8(b) and 8(c)). It is evident from these results that the polymerized NOA65 contributed to signal amplification and significantly improved the LOD, which was an order of magnitude lower for the AY40-006/NOA65 film with the target CA125 protein captured by antibodies of $10^{-2}$ fold of that for the AY40-006 film.

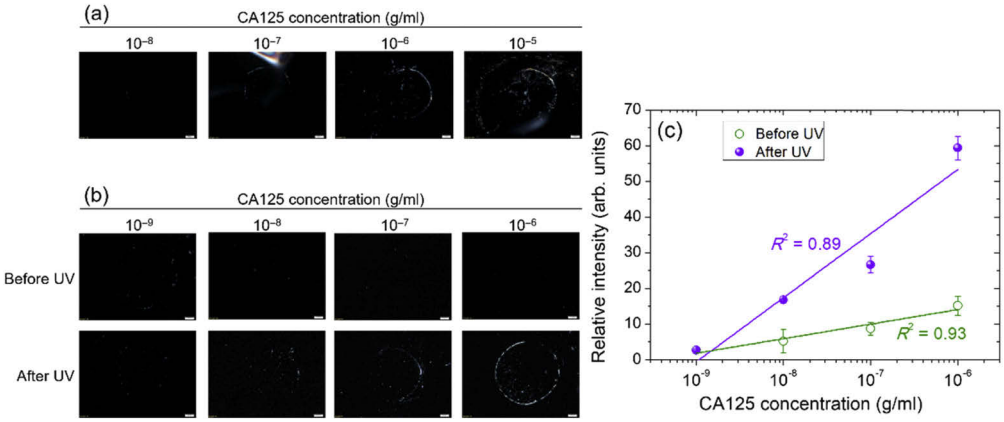


**Fig. 8.** Optical textures of the LC and LC–photopolymer composite films in the presence of various concentrations of CA125 and the corresponding quantitative results. Anti-CA125 antibodies were immobilized on the DMOAP-coated glass substrate at a concentration of (a) 0.01 $\mu$g/ml or (b) 0.1 ng/ml, followed by immunoreaction with various concentrations of CA125. The immunocomplex was detected with a spin-coated film of (a) AY40-006 without UV exposure or (b) AY40-006 dispersed with 4-wt% NOA65 followed by UV irradiation at 15 mW/cm$^2$ for 30 s. Scale bar: 100 $\mu$m. (c) Quantitative results from image analysis of the optical textures with the GIMP software are expressed as relative intensities against the CA125 concentration. Error bars represent standard deviations calculated from the relative intensities of at least three independent experiments. Solid lines represent the fitted linear regression lines, with the coefficient of determination, $R^2$, indicated in the same color.

Proteins absorb UV radiation at wavelengths around 280 nm through the aromatic amino acids tryptophan, tyrosine and phenylalanine. As a reference, common experimental conditions for UV crosslinking of protein to DNA requires UV irradiation for 5–60 min from 5 cm above the sample with a UV transilluminator of 305 nm at an intensity of 7 mW/cm$^2$ [26]. In addition, exposure to UV light of 365 nm in wavelength at an intensity of 5–20 mW/cm$^2$ for 2–20 min is considered non-cytotoxic to cells [27]. Although we cannot conclude whether the long-wave UV light (365 nm) used in this study affected the structure and activity of the CA125 protein or anti-CA125 antibody, the outcome of the CA125 immunoassay was unaltered by UV exposure because the part of the biosensing procedure that required the protein structure and activity to be intact was accomplished prior to spin-coating of the LC–photopolymer composite film. The CA125 protein and anti-CA125 antibody need not be active after UV irradiation as long as it was adsorbed to the DMOAP-coated glass substrate. Consequently, the LC-based single-substrate biosensing method proposed here is an end-point assay, as opposed to continuous assays or real-time detection. Nevertheless, unless the kinetics of the biomolecular interaction is critical to analysis or diagnosis, end-point assays simplify the design of the biosensor and fulfill the requirements of most fast-screening and point-of-care devices.

Biomedical Optics EXPRESS

### 3.4. Comparison between LC-based single-substrate and LC-cell bioassay platforms

We have previously established an LC-based CA125 immunodetection platform by sandwiching a nematic film of ~5.1 $\mu$m between a pair of DMOAP-coated glass substrates to form an LC cell [19]. This allowed BSA and CA125 to be detected by a nematic of high birefringence, HDN ($\Delta n = 0.333$ at 589.3 nm and 20 °C; nematic temperature range: < −30–95 °C), at a minimal concentration of $10^{-11}$ g/ml BSA and $10^{-8}$ g/ml CA125 when 0.1 $\mu$g/ml anti-CA125 antibody (0.1 ng/spot at 1 $\mu$l/spot in a $3 \times 3$ antibody array) was immobilized on the glass substrate. Employing high-birefringence and wide-nematic-range HDN was one of our approaches toward signal amplification of LC-based label-free detection. It significantly ameliorated the detection limit compared with that enabled by the conventional biosensing mesogen 5CB ($\Delta n = 0.179$ at 589.3 nm and 25 °C) that grants a very narrow workable temperature range of 11 °C (as determined by the nematic temperature range of 24–35 °C) [18–20]. In this study the LOD for BSA and CA125 were $1.6 \times 10^{-12}$ and $2.1 \times 10^{-8}$ g/ml, respectively, in single-substrate detection when a filmy composite formed by AY40-006 containing 4-wt% NOA65 exposed to 15-mW/cm$^2$ UV radiation was applied as a transducer. Although AY40-006 has a smaller birefringence than HDN, single-substrate detection assisted with polymerized NOA65 brought about a detection limit comparable to that of HDN in LC cells, with easier sample fabrication and significantly less capture antibody required in the CA125 immunoassay.

## 4. Conclusions

A novel signal amplification approach for label-free LC-based biosensing has been demonstrated by utilizing a UV-cured LC–prepolymer film on a single glass substrate. The amount of the NOA65 prepolymer and the level of photopolymerization were critical to the morphology of the resulting photopolymer accumulated at the LC–glass interface and, in turn, to signal amplification. We optimized the synthetic procedure of the LC–photopolymer composite film to minimize the background signal in the absence of the target of detection, and to amplify the optical signal derived from biomolecules to lower the LOD. It was observed that, by spin-coating a ~4.5-$\mu$m thin film consisting of AY40-006 mixed with 4-wt% NOA65 followed by UV irradiation at 15 mW/cm$^2$ for 30 s, a LOD of $1.6 \times 10^{-12}$ g/ml for BSA and $2.1 \times 10^{-8}$ g/ml for CA125 can be unambiguously achieved, which was significantly lower than biodetection with AY40-006 alone or with the AY40-006/NOA65 mixture prior to UV-induced polymerization. Compared with conventional LC-based biosensing techniques utilizing LC cells assembled with two glass substrates, the single-substrate biosensing platform can be more easily integrated with microarray technologies to facilitate high-throughput screening and analysis, and can be further applied in the detection of protein–protein, protein–peptide, and protein–DNA interactions, as well as DNA hybridization assays. The label-free single-substrate biosensing technology reported in the present study provides the first implication on the biomedical application of LC–photopolymer composites, leading to a new prospect for LC-based single-substrate biosensors for the development of simple and fast-screening point-of-care devices.

## Funding

Ministry of Science and Technology, Taiwan (107-2112-M-009-012-MY3, 109-2320-B-309-001).

## Disclosures

The authors declare that there are no conflicts of interest related to this article.

## References

1. R. J. Carlton, J. T. Hunter, D. S. Miller, R. Abbasi, P. C. Mushenheim, L. N. Tan, and N. L. Abbott, "Chemical and biological sensing using liquid crystals," Liq. Cryst. Rev. **1**(1), 29–51 (2013).

Biomedical Optics EXPRESS


2. S. L. Helfinstine, O. D. Lavrentovich, and C. J. Woolverton, "Lyotropic liquid crystal as a real-time detector of microbial immune complexes," Lett. Appl. Microbiol. **43**(1), 27–32 (2006).
3. P. Popov, E. K. Mann, and A. Jakli, "Thermotropic liquid crystal films for biosensors and beyond," J. Mater. Chem. B **5**(26), 5061–5078 (2017).
4. M.-J. Lee and W. Lee, "Liquid crystal-based capacitive, electro-optical and dielectric biosensors for protein quantitation," *Liq. Cryst.* 1. (2019).
5. D.-K. Yang, L.-C. Chien, and Y. K. Fung, "Polymer-stabilized Cholesteric Textures: Materials and Applicaiotns," in *Liquid Crystals in Complex Geometries*, edited by G. P. Crawford and S. Zumer eds., (Taylor and Francis, 1996), Chap. 4, p. 106.
6. Y. Zhang, C. Wang, W. Zhao, M. Li, X. Wang, X. Yang, X. Hu, D. Yuan, W. Yang, Y. Zhang, P. Lv, J. He, and G. Zhou, "Polymer stabilized liquid crystal smart window with flexible substrates based on low-temperature treatment of polyamide acid technology," Polymers **11**(11), 1869 (2019).
7. H. Kikuchi, M. Yokota, Y. Hisakado, H. Yang, and T. Kajiyama, "Polymer-stabilized liquid crystal blue phases," Nat. Mater. **1**(1), 64–68 (2002).
8. J. Yuan, G. Tan, D. Xu, F. Peng, A. Lorenz, and S.-T. Wu, "Low-voltage and fast-response polymer-stabilized hyper-twisted nematic liquid crystal," Opt. Mater. Express **5**(6), 1339–1347 (2015).
9. H. Mehrzad, E. Mohajerani, K. Neyts, and M. Mohammadimasoudi, "Polymer dispersed liquid crystal-mediated active plasmonic mode with microsecond response time," Opt. Lett. **44**(5), 1088–1091 (2019).
10. P.-C. Wu, H.-L. Chen, N. V. Rudakova, I. V. Timofeev, V. Y. Zyryanov, and W. Lee, "Electro-optical and dielectric properties of polymer-stabilized blue phase liquid crystal impregnated with a fluorine-containing compound," J. Mol. Liq. **267**, 138–143 (2018).
11. Z.-Y. Kuang, Y. Deng, J. Hu, L. Tao, P. Wang, J. Chen, and H.-L. Xie, "Responsive smart windows enabled by the azobenzene copolymer brush with photothermal effect," ACS Appl. Mater. Interfaces **11**(40), 37026–37034 (2019).
12. F. P. Nicoletta, G. Chidichimo, D. Cupelli, G. De'Filpo, M. De'Benedittis, B. Gabriele, G. Salerno, and A. Fazio, "Electrochromic polymer-dispersed liquid-crystal film: a new bifunctional device," Adv. Funct. Mater. **15**(6), 995–999 (2005).
13. C.-M. Lin, P.-C. Wu, M.-J. Lee, and W. Lee, "Label-free protein quantitation by dielectric spectroscopy of dual-frequency liquid crystal," Sens. Actuators, B **282**, 158–163 (2019).
14. W.-L. Hsu, M.-J. Lee, and W. Lee, "Electric-field-assisted signal amplification for label-free liquid-crystal-based detection of biomolecules," Biomed. Opt. Express **10**(10), 4987–4998 (2019).
15. C.-H. Lin, M.-J. Lee, and W. Lee, "Bovine serum albumin detection and quantitation based on capacitance measurements of liquid crystals," Appl. Phys. Lett. **109**(9), 093703 (2016).
16. P.-C. Wu, A. Karn, M.-J. Lee, W. Lee, and C.-Y. Chen, "Dye-liquid-crystal-based biosensing for quantitative protein assay," Dyes Pigm. **150**, 73–78 (2018).
17. M.-J. Lee, C.-H. Lin, and W. Lee, "Liquid-crystal-based biosensing beyond texture observations," Proc. SPIE **9565**, 956510 (2015).
18. H.-W. Su, M.-J. Lee, and W. Lee, "Surface modification of alignment layer by ultraviolet irradiation to dramatically improve the detection limit of liquid-crystal-based immunoassay for the cancer biomarker CA125," J. Biomed. Opt. **20**(5), 057004 (2015).
19. H.-W. Su, Y.-H. Lee, M.-J. Lee, Y. C. Hsu, and W. Lee, "Label-free immunodetection of the cancer biomarker CA125 using high-Δn liquid crystals," J. Biomed. Opt. **19**(7), 077006 (2014).
20. S.-H. Sun, M.-J. Lee, Y.-H. Lee, W. Lee, X. Song, and C.-Y. Chen, "Immunoassays for the cancer biomarker CA125 based on a large-birefringence nematic liquid-crystal mixture," Biomed. Opt. Express **6**(1), 245–256 (2015).
21. Y.-L. Chiang, M.-J. Lee, and W. Lee, "Enhancing detection sensitivity in quantitative protein detection based on dye-doped liquid crystals," Dyes Pigm. **157**, 117–122 (2018).
22. H. Kang, J. M. Lee, J.-H. Kim, J.-H. Lee, J. S. Park, J. G. Seo, and D. Kang, "Homeotropic alignment properties of liquid crystal and photocurable monomer system via UV irradiation," Mol. Cryst. Liq. Cryst. **606**(1), 101–110 (2015).
23. C.-J. Hsu, B.-L. Chen, and C.-Y. Huang, "Controlling liquid crystal pretilt angle with photocurable prepolymer and vertically aligned substrate," Opt. Express **24**(2), 1463–1471 (2016).
24. R. D. Deegan, O. Bakajin, T. F. Dupont, G. Huber, S. R. Nagel, and T. A. Witten, "Capillary flow as the cause of ring stains from dried liquid drops," Nature **389**(6653), 827–829 (1997).
25. A. Shrivastava and V. Gupta, "Methods for the determination of limit of detection and limit of quantitation of the analytical methods," Chron. Young Sci. **2**(1), 21–25 (2011).
26. L. A. Chodosh, "UV crosslinking of proteins to nucleic acids," Curr. Protoc. Mol. Biol. **36**(1), 12 (1996).
27. D.Y. Wong, T. Ranganath, and A. M. Kasko, "Low-dose, long-wave UV light does not affect gene expression of human mesenchymal stem cells," PLoS One **10**(9), e0139307 (2015).